A Convex Optimization Framework for Regularized Geodesic Distances - Supplemental Material

Michal Edelstein
Technion - Israel Institute of Technology
Haifa, Israel
smichale@cs.technion.ac.il

Nestor Guillen
Texas State University
San Marcos, TX, USA
nestor@txstate.edu

Justin Solomon
Massachusetts Institute of Technology (MIT)
Cambridge, MA, USA
jsolomon@mit.edu

Mirela Ben-Chen
Technion - Israel Institute of Technology
Haifa, Israel
mirela@cs.technion.ac.il

ACM Reference Format:
Michal Edelstein, Nestor Guillen, Justin Solomon, and Mirela Ben-Chen. 2023. A Convex Optimization Framework for Regularized Geodesic Distances - Supplemental Material. In *Special Interest Group on Computer Graphics and Interactive Techniques Conference Conference Proceedings (SIGGRAPH '23Conference Proceedings), August 6–10, 2023, Los Angeles, CA, USA.* ACM, New York, NY, USA, 8 pages. https://doi.org/10.1145/3588432.3591523

1 PROOFS REGARDING ANALYTICAL SOLUTIONS (SECTION 3.1)

In this section we justify the formulas for the solutions to the problems in Section 3.1. Essential to these computations is the obstacle problem. For flat geometries or for general M but with α sufficiently small, the solution to problem (3) is the same as the solution to *the obstacle problem with obstacle given by* $d(x, E)$. The obstacle problem in this case takes the form

$$\boxed{\begin{array}{ll} \text{Minimize}_u & \alpha\mathcal{E}(u) - \int_M u(x)\ \mathrm{dVol}(x) \\ \text{subject to} & u(x) \leq d(x,E) \text{ for all } x \in M. \end{array}} \tag{S1}$$

The equivalence between this problem and problem (3) is a classical fact in the case where M is an open domain of $\mathbb{R}^n$ and $E = \partial M$, in this classical setting problem (3) is known as the elastic-plastic torsion problems. The equivalence in the situation M is a Riemannian manifold is a more recent result and can be found in [Générau et al . 2022].In the general Riemannian case the equivalence between problem (3) and the obstacle problem might not hold for all values of α, but it will hold for all α smaller than some $\alpha_0 = \alpha_0(M)$.

1.1 Analytical solution for the circle

We now prove the formula for the solution to the minimization problem in the case of $M = \mathbb{S}^1$ (Section 3.1). Recall that in Section 3.1 we have identified $\mathbb{S}^1$ with the real numbers modulo 2π.

SIGGRAPH '23 Conference Proceedings, August 6–10, 2023, Los Angeles, CA, USA

ACM ISBN 979-8-4007-0159-7/23/08.
https://doi.org/10.1145/3588432.3591523

We claimed the solution where the source point is at $x = 0$ is given by the formula

$$u_\alpha(x) = \begin{cases} \hat{x} & \text{if } 0 \leq \hat{x} \leq L \\ \pi - \frac{1}{2}\alpha - \frac{1}{2\alpha}(\hat{x} - \pi)^2 & \text{if } L \leq \hat{x} \leq 2\pi - L \\ 2\pi - \hat{x} & \text{if } \hat{x} \geq L \end{cases} \tag{5}$$

(recall $\hat{x}$ is the unique representative of x in the interval $[0, 2\pi)$ modulo 2π), where $L(\alpha)$ is given by

$$L(\alpha) = (\pi - \alpha)_+. \tag{6}$$

We are going to show the function u_α is a solution to the obstacle problem (S1), which in this case reduces to

$$\boxed{\begin{array}{ll} \text{Minimize}_u & \alpha \int_0^{2\pi} |u'|^2\ dx - \int_0^{2\pi} u(x)\ dx \\ \text{subject to} & u(x) \leq d(x,0) \text{ for all } x \in [0, 2\pi] \end{array}} \tag{S2}$$

The function $d(x, 0)$ for $x \in [0, 2\pi]$ is equal to

$$d(x, 0) = \min\{|x|, |x - 2\pi|\} = \pi - |x - \pi|.$$

The classical theory for the obstacle problem (see [Petrosyan et al. 2012]) says that if a function u is of class $C^{1,1}$ in the entire domain (i.e. its gradient is Lipschitz continuous), is of class C^2 in the interior of $\{u < d(x, 0)\}$, and solves

$$\alpha u'' + 1 \geq 0 \text{ in the sense of distributions,}$$
$$\alpha u'' + 1 = 0 \text{ in the interior of } \{u < d(x, 0)\},$$

then that function u will be the solution to the obstacle problem (S2). Let us verify this in our current example. First, by direct computation we can see u has a continuous derivative in $(0, 2\pi)$, and

$$u'(x) = \begin{cases} 1 & \text{if } 0 \leq \hat{x} \leq L \\ -\frac{1}{\alpha}(x - \pi) & \text{if } L \leq \hat{x} \leq 2\pi - L \\ -1 & \text{if } \hat{x} \geq L \end{cases} \tag{S3}$$

We emphasize this function is continuous even at $x = L, 2\pi - L$. Next, this function is twice differentiable away from $x = L, 2\pi - L$ and in particular it is twice differentiable in the set $\{u < d(x, 0)\} = (L, 2\pi - L)$. We have

$$u''(x) = \begin{cases} 0 & \text{if } 0 \leq \hat{x} < L \\ -\frac{1}{\alpha} & \text{if } L < \hat{x} < 2\pi - L \\ 0 & \text{if } \hat{x} > L \end{cases} \tag{S4}$$

This shows that $\alpha u'' + 1 = 0$ in $\{u < d(x, 0)\}$. Lastly, since u is differentiable everywhere this means that as a measure the function u'' is equal to $-(1/\alpha)\chi_{(L,2\pi-L)}(x)$, χ denoting the indicator function. It follows that $\alpha u'' + 1 \geq 0$ in the sense of distributions. This proves that u is indeed the solution to the obstacle problem, and in turn, of problem (3) in the case $M = \mathbb{S}^1$ and $E = \{0\}$.

That is, the function u_α is of class C^2 away from $x = L, 2\pi - L$ and u''_α is continuous everywhere except at $L, 2\pi - L$. From here follows that $\alpha u''_\alpha + 1$ is well defined as a measure, and that always ≥ 0 and is exactly zero in the interval $(L, 2\pi - L)$. This shows that u_α solves

$$\min\{\alpha u''_\alpha + 1, (\pi - |x - \pi|) - u_\alpha\} = 0.$$

Lastly, we prove the function $u_\alpha(x, y)$ is indeed a metric.

1.2 Proof that $u_\alpha(x, y)$ is a metric in $\mathbb{S}^1$

By definition, we have $u_\alpha(x, y) = u_\alpha(x - y)$ where $u_\alpha(x)$ is as in (5). From here follows that $u_\alpha(x, y) \geq 0$ for all x, y, since the function in (5) is non-negative. Moreover, the function in (5) only vanishes at x equal to an integer multiple of 2π (since in that case $\hat{x} = 0$, per the definition of $\hat{x}$), therefore $u_\alpha(x, y) = 0$ only if $x - y$ is a multiple of 2π, i.e. only if x and y correspond to the same point in $\mathbb{S}^1$.

To prove symmetry, simply observe that in (5) we have $u_\alpha(x) = u_\alpha(-x)$, so $u_\alpha(x - y) = u_\alpha(y - x)$.

It remains to show $u_\alpha(x, y)$ satisfies the triangle inequality. That is, we have to prove that for any x, y, z we have

$$u_\alpha(x - y) \leq u_\alpha(x - z) + u_\alpha(z - y).$$

By translation invariance (i.e. by symmetry) we may assume without loss of generality that $z = 0$. Then, all we have to prove is that for all x, y we have

$$u_\alpha(x - y) \leq u_\alpha(x) + u_\alpha(-y).$$

Now, fix y and consider the function

$$v(x) := u_\alpha(x - y) - u_\alpha(-y).$$

What we want to prove amounts to the inequality $v(x) \leq u_\alpha(x)$. The function $v(x)$ satisfies the inequality

$$v(x) \leq d(x, 0), \quad \text{for all } x,$$

as well as the differential inequality

$$\alpha v'' + 1 \geq 0.$$

One well known characterization of the function $u_\alpha(x)$ is that it is the largest function having these two properties. In this case we conclude that $u_\alpha(x) \geq v(x)$, and the triangle inequality is proved.

1.3 Analytical solution for the disk

To illustrate how our method handles other choices for the source set E, we take the flat 2D disk and consider the regularized distance to the boundary of the disk.

Using polar coordinates, we take $E = \{(r, \theta) | r = R\}$, and minimize

$$\frac{\alpha}{2}\int_0^R \int_0^{2\pi} |\nabla u(r, \theta)|^2 \, d\theta dr - \int_0^R \int_0^{2\pi} u(r, \theta) r \, d\theta dr$$

with the constraints

$$u(R, \theta) \leq 0 \text{ for all } \theta \in [0, 2\pi], \text{ and}$$
$$|\nabla u(r, \theta)| \leq 1 \text{ for all } r \in [0, R), \theta \in [0, 2\pi].$$

In this case, the solution is:

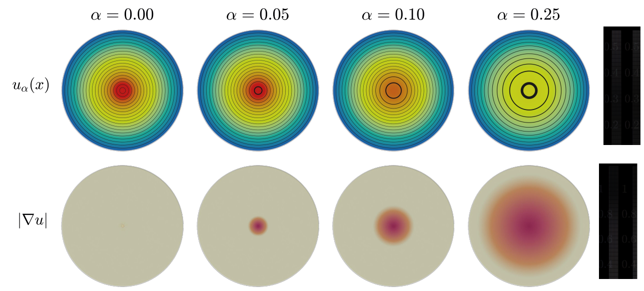

Figure 1: The analytical solution for the regularized geodesic distance using the Dirichlet regularizer on the disk (top). We also display the gradient norm, $|\nabla u|$ (bottom). Note the different smoothing regions, whose width depends on α.

$$u_\alpha(x) = \begin{cases} -\frac{1}{4\alpha}|x|^2 + R - \alpha & \text{if } |x| \leq 2\alpha \\ R - |x| & \text{if } 2\alpha < |x| \leq R \end{cases} \tag{S5}$$

To prove this formula, we proceed similarly to the case of $\mathbb{S}^1$. This function is of class $C^{1,1}$, first note that its gradient is given by

$$\nabla u_\alpha(x) = \begin{cases} -\frac{1}{2\alpha}x & \text{if } |x| \leq 2\alpha \\ -\frac{x}{|x|} & \text{if } 2\alpha < |x| \leq R \end{cases}$$

and this vector-valued function is continuous across $|x| = 2\alpha$ (in fact, it is Lipscthiz continuous). Moreover, for the Laplacian of u_α we have

$$\Delta u_\alpha(x) = \begin{cases} -\frac{1}{\alpha} & \text{if } |x| \leq 2\alpha \\ -\frac{1}{|x|} & \text{if } 2\alpha < |x| \leq R \end{cases}$$

Accordingly, $\alpha \Delta u_\alpha + 1 \geq 0$ everywhere in the disk $\{|x| < R\}$ and $\alpha \Delta u_\alpha + 1 = 0$ exactly when $u_\alpha < d(x, E) = R - |x|$. From here we conclude that the function u_α given by (S5) is the solution.

Figure 1 shows the behavior of the function on the disk. Observe that as in the case of the circle, the solution has two regimes, one where it matches the distance function exactly, and one where it solves Poisson's equation $\Delta u = -1/\alpha$. In this case, this results in the cone singularity being replaced by a concave quadratic function that is differentiable and only has a discontinuity in its second derivative.

2 EXISTENCE AND UNIQUENESS OF THE MINIMIZER (SECTION 3)

In our results, M is a compact C^∞ submanifold of N-dimensional Euclidean space $\mathbb{R}^N$, from where it inherits its Riemannian structure. The function $F(\xi, x)$, $F : \mathbb{R}^N \times \mathbb{R}^N \to \mathbb{R}$ is assumed of class C^1 in (ξ, x). We make two further structural assumptions on F:
1) There are $p > 1$ and c_0, C_0 positive such that

$$c_0|\xi|^p \leq F(\xi, x) \leq C_0|\xi|^p, \quad \forall\, x, \xi \in \mathbb{R}^N$$

2) The function F is strictly convex in the first argument. This is meant in the following sense: given vectors $\xi_1 \neq \xi_2$ and $s \in (0, 1)$ then we have the strict inequality for all x

$$F((1 - s)\xi_1 + s\xi_2, x) < (1 - s)F(\xi_1, x) + sF(\xi_2, x).$$

From these assumptions follows in particular that $F(\xi, x) \geq 0$ for all ξ and x, and $F(\xi, x) = 0$ only if $\xi = 0$. Observe that these assumptions include all F's of the forms

$$F(\xi, x) = |A(x)\xi|^p$$

where $p > 1$ and $A(x)$ is a smooth positive definite matrix whose eigenvalues are uniformly bounded away from zero and infinity.

Now we prove the existence and uniqueness for the general minimization problem. The problem (see problem (3)) is a constrained minimization problem in the Sobolev space $W^{1,p}(M)$.

$$\boxed{\begin{array}{rl} \text{Minimize}_u & \alpha \int_M F(\nabla u, x)\ \text{dVol}(x) - \int_M u\ \text{dVol}(x) \\ \text{subject to} & u \in W^{1,p}(M) \\ & |\nabla u(x)| \leq 1 \text{ for all } x \in M \setminus E \\ & u(x) \leq 0 \text{ for all } x \in E. \end{array}} \quad (3)$$

The space $W^{1,p}(M)$ $(1 \leq p < \infty)$ is defined as follows

$$W^{1,p}(M) := \left\{ u : M \to \mathbb{R} \ \middle|\ \begin{array}{l} \nabla u \text{ exists as a distribution} \\ \int_M |u|^p + |\nabla u|^p\ dx < \infty \end{array} \right\}$$

Here, $E \subset M$ is a non-empty closed subset of M. For us, the case of chief interest is when $E = \{x_0\}$ for a given $x_0 \in M$.

In what follows, we will denote the objective functional by J_α,

$$J_\alpha(u) := \alpha \int_M F(\nabla u, x)\ \text{dVol}(x) - \int_M u\ \text{dVol}(x)$$

We now prove the existence and uniqueness first theorem stated in Section 3.

Theorem 3.1. *There is a unique minimizer for problem (3).*

Proof. Consider a minimizing sequence $\{u_k\}_k$. First, we claim that without loss of generality, we can assume that for each k,

$$\max_M u_k \geq 0. \quad \text{(S7)}$$

Indeed, if for some k_0 we had u_{k_0} is non-positive in all of M, it would follow that

$$J_\alpha(u_{k_0}) \geq 0 = J_\alpha(0).$$

Thus the minimizing sequence will remain a minimizing sequence if we replace every non-positive element of the sequence with the zero function.

Henceforth, we assume our sequence u_k is such that (S7) holds for all k. In this case, as the u_k are all 1-Lipschitz, it follows that

$$u_k(x) \geq \max_M u_k(x) - \text{diam}(M) \geq -\text{diam}(M) \text{ for all } k.$$

A similar argument—using that $\max_{x\in E} u_k(x) \leq 0$ for all k—provides the inequality in the opposite direction. In conclusion,

$$\|u_k\|_{L^\infty(M)} \leq \text{diam}(M) \ \text{ for all } k.$$

It follows that the sequence $\{u_k\}_k$ is 1-Lipschitz and uniformly bounded. Then, by the Arzela-Ascoli theorem there is a subsequence u'_k and a function u_* in M such that

$$\|u'_k - u_*\|_{L^\infty(M)} \to 0 \text{ as } k \to \infty.$$

Moreover, without loss of generality (we can always pass to another subsequence where this holds)) we also have

$$\nabla u'_k \to \nabla u_* \text{ in weak-}L^p(M).$$

In particular,

$$\lim_k \int_M u'_k(x)\ \text{dVol}(x) = \int_M u_*(x)\ \text{dVol}(x).$$

In this case, due to the weak convergence of $\nabla u'_k$, as well as the convexity of F in the first argument and its two-sided pointwise bounds, we conclude that

$$\liminf_k \int_M F(\nabla u'_k, x)\text{dVol}(x) \geq \int_M F(\nabla u_*, x)\text{dVol}(x)$$

Putting everything together, we ahve shown that

$$\liminf_k J_\alpha(u'_k) \geq J_\alpha(u_*).$$

Since the 1-Lipschitz constraint as well as the constraint $u_k(x) \leq 0$ for all $x \in E$ are preserved by the uniform convergence, it follows that u_* is admissible. Moreover, the last liminf inequality says u_* achieves the minimum of J_α among all admissible functions, so u_* is a minimizer for the problem.

The uniqueness follows from the strict convexity through a standard argument, which we review for completeness: suppose there are two separate minimizers u_0 and u_1. For each $s \in [0, 1]$ let

$$u_s = (1 - s)u_0 + su_1.$$

From the convexity assumption on F we know that

$$F(\nabla u_s, x) \leq (1 - s)F(\nabla u_0, x) + sF(\nabla u_1, x).$$

In terms of the functional, this gives us

$$J_\alpha(u_s) \leq (1 - s)J_\alpha(u_0) + J_\alpha(u_1)$$

by merely integrating the pointwise inequality, and at the same time

$$J_\alpha(u_s) \geq (1 - s)J_\alpha(u_0) + J_\alpha(u_1)$$

Since u_0 and u_1 are minimizers and u_s is admissible for every $s \in [0, 1]$. This can only happen if

$$F(\nabla u_s, x) = (1 - s)F(\nabla u_0, x) + sF(\nabla u_1, x)\ \forall\ x \in M,$$

and by the assumption, this can only happen if $\nabla u_0 = \nabla u_1$ at every x. As u_0 and u_1 have to agree at least at one point, x_0, this means that $u_0 = u_1$. □

3 CONVERGENCE TO THE GEODESIC DISTANCE (SECTION 3)

In this section we prove the convergence theorem from Section 3.

Theorem 3.2. *The functions u_α converge uniformly to $d(\cdot, E)$,*

$$\|u_\alpha - d(\cdot, E)\|_{L^\infty} \to 0 \text{ as } \alpha \to 0^+.$$

Proof. We make use of an elementary but often used fact in nonlinear PDE that says that compactness plus uniqueness of the limiting points of a sequence in turn guarantees convergence of the whole sequence.[1] Concretely, and in two parts, we are going to show 1) that given any sequence $\alpha_k \to 0^+$ we can pass to a subsequence α'_k which converges uniformly to some function u_*

$$\|u_{\alpha'_k} - u_*\|_{L^\infty(M)} \to 0 \text{ as } k \to \infty,$$

[1] if the sequence failed to converge as whole, there would be some $\delta > 0$ an infinite subsequence such that $u_{\alpha'_k}$ stays a distance at least δ from $d(x, x_0)$, leading to a contradiction

and subsequently that 2) whatever function u_* is obtained as one of these limits will have to be a minimizer for problem (1). Since that problem has as its unique solution, then $u_* = d(x, x_0)$ for all such subsequences.

Indeed, first, note that the 1-Lipschitz constraint and the fact that $u_{\alpha_k}(x_0) = 0$ for all k implies that the sequence u_{α_k} lies in a compact subset of $C(M)$. Therefore, there is a subsequence α_k' and a 1-Lipschitz function $u_* \in C(M)$ such that

$$u_{\alpha_k'} \to u_* \text{ uniformly in } M.$$

Now, let $\phi : M \to \mathbb{R}$ be a 1-Lipschitz function such that $\phi(x_0) \le 0$. Since ϕ is admissible for (3) for every α_k', it follows that

$$\begin{aligned} -\int_M u_{\alpha_k'} \mathrm{dVol}(x) &\le \alpha_k' \int_M F(\nabla u_{\alpha_k'}, x)\mathrm{dVol}(x) - \int_M u_{\alpha_k'}\, dx \\ &\le \alpha_k' \int_M F(\nabla\phi, x)\mathrm{dVol}(x) - \int_M \phi\, dx. \end{aligned}$$

On the other hand, by the 1-Lipschitz constraint

$$\int_M F(\nabla\phi, x)\mathrm{dVol}(x) \le C\mathrm{Vol}(M).$$

This means in particular that

$$\begin{aligned} -\int_M u_* \mathrm{dVol(x)} &= \lim_k \int_M u_{\alpha_k'} \mathrm{dVol}(x) \\ &\le \lim_k \left\{ \alpha_k' \int_M F(\nabla\phi, x)\mathrm{dVol}(x) - \int_M \phi\, dx \right\} \\ &= -\int_M \phi(x)\, dx. \end{aligned}$$

This shows that u_* solves the minimization problem (1), and this problem has a known solution, so $u_* = d(\cdot, E)$. In summary we have shown that given any sequence $\alpha_k \to 0$ there is a subsequence α_k' such that $u_{\alpha_k'} \to d(\cdot, E)$ uniformly in M, finishing the proof. □

4 ANALYTICAL SOLUTION FOR THE HESSIAN REGULARIZER IN 1D (HESSIAN REGULARIZER, SECTION 4.2)

In $1D$, the Hessian energy is the same as the bilaplacian energy, and the optimization problem is:

$$\begin{array}{rl} \text{Minimize}_u & \frac{\alpha}{2}\int_0^{2\pi} |u''(x)|^2\, \mathrm{d}x - \int_0^{2\pi} u(x)\, \mathrm{d}x \\ \text{subject to} & |u'(x)| \le 1 \text{ for all } x \in (0, 2\pi) \\ & u(0) \le 0. \end{array}$$

The minimizer $u(x)$ is (for $x \in [0, 2\pi]$):

$$u(x) = \begin{cases} x & \text{if } 0 \le x \le \pi - c \\ \frac{1}{24\alpha}(x-\pi)^4 - \frac{c^2}{4\alpha}(x-\pi)^2 \\ \quad +\pi - c + \frac{5c^4}{24\alpha} & \text{if } \pi - c \le x \le \pi + c \\ 2\pi - x & \text{if } x \ge \pi + c \end{cases}$$

where $c = \sqrt[3]{3\alpha}$.

Note that the function and smoothing region are different than the ones in the Dirichlet regularizer case.

5 EXISTENCE AND UNIQUENESS OF A MINIMIZER (PRODUCT MANIFOLD FORMULATION, SECTION 6)

In Section 6 we introduced the following problem.

$$\begin{array}{rl} \text{Minimize} & \alpha\mathcal{E}_{M\times M}(U) - \int_{M\times M} U(x,y)\ \mathrm{dVol}(x,y) \\ \text{subject to} & U \in W^{1,2}(M\times M) \\ & |\nabla_1 U(x,y)| \le 1 \text{ in } \{(x,y) \mid x \ne y\} \\ & |\nabla_2 U(x,y)| \le 1 \text{ in } \{(x,y) \mid x \ne y\} \\ & U(x,y) \le 0 \text{ on } \{(x,y) \mid x = y\} \end{array} \tag{12}$$

Theorem 6.1. *There is a unique minimizer in problem* (12).

Proof. At the big picture level this proof is basically the same as that of existence and uniqueness of a minimizer for problem (3). We only highlight the points where things are different.

Therefore, take a minimizing sequence U_k. Arguing similarly as before we can assume without loss of generality that

$$\max_{M\times M} U_k \ge 0 \text{ for all } k.$$

Now, U_k is 1-Lipschitz in each variable x and y, separately, so, if for some k (x_0, y_0) is a point where $U_k(x_0, y_0) \ge 0$, then for all other (x, y) we have

$$\begin{aligned} U_k(x,y) &\ge U_k(x, y_0) - d(y, y_0) \\ &\ge U_k(x_0, y_0) - d(x, x_0) - d(y, y_0) \\ &\ge U_k(x_0, y_0) - 2\mathrm{diam}(M). \end{aligned}$$

On the other hand, since $U_k(x, x) \le 0$ for all x and y, we have, using the 1-Lipschtz condition in the first variable

$$\begin{aligned} U_k(x,y) &\le U_k(x,x) + d(x,y) \\ &\le d(x,y) \le \mathrm{diam}(M). \end{aligned}$$

Putting all this together we have

$$\|U_k\|_{L^\infty(M)} \le 2\mathrm{diam}(M) \text{ for all } k.$$

This means our sequence $\{U_k\}_k$ is uniformly bounded and equicontinuous (in fact, uniformly Lipschitz) in the compact space $M \times M$.

By the Arzela-Ascoli theorem, there is a subsequence U_k' and a function U_* in $M \times M$ such that U_k converges uniformly to U_*. In particular, this function U_k will be Lipschitz and the inequalities

$$|\nabla_1 U_*(x,y)| \le 1 \text{ and } |\nabla_2 U_*(x,y)|$$

hold for a.e. $(x, y) \in M \times M$. Moreover, $U_*(x, x) \le 0$ for all $x \in M$. This shows that U_* is admissible for problem (12). At the same time, the uniform convergence of the U_k and the compactness of $M \times M$ imply that

$$\lim_k \int_{M\times M} U_k'(x,y)\mathrm{dVol}(x,y) = \int_{M\times M} U_*(x,y)\mathrm{dVol}(x,y).$$

Lastly, passing to another subsequence U_k'' if needed, we have

$$\begin{aligned} &\liminf_k \int_{M\times M} |\nabla_1 U_k''|^2 + |\nabla_2 U_k''|^2 \mathrm{dVol}(x,y) \\ &\ge \int_{M\times M} |\nabla_1 U_*|^2 + |\nabla_2 U_*|^2 \mathrm{dVol}(x,y). \end{aligned}$$

From here it follows that U_* is a minimizer for problem (12).

Uniqueness is proved again making use of the convexity of the functional.

□

A consequence of the uniqueness theorem is the symmetry of the minimizers U_α:

Theorem 6.2. *The function $U_\alpha(x, y)$ is symmetric in x and y.*

Proof. This is a direct consequence of the uniqueness of the minimizer to problem (12) as well as the symmetry of the under the transformation $(x, y) \mapsto (y, x)$. Indeed, given α define the function

$$v_\alpha(x, y) := U_\alpha(y, x),$$

Then it is clear that v is still admissible for problem (12) and

$$\alpha \mathcal{E}_{M\times M}(U_\alpha) - \int_{M\times M} U_\alpha(x, y)\ \mathrm{dVol}(x, y)$$
$$= \alpha \mathcal{E}_{M\times M}(v) - \int_{M\times M} v(x, y)\ \mathrm{dVol}(x, y),$$

so that v also achieves the minimum of problem (12). Since there is only one minimizer, $v = U_\alpha$ and the lemma follows. □

6 CONVERGENCE TO THE FULL GEODESIC DISTANCE (PRODUCT MANIFOLD FORMULATION, SECTION 6)

In this section we will make use of the following characterization of the geodesic distance function $d(x, y)$.

$$\boxed{\begin{array}{ll} \text{Minimize} & -\int_{M\times M} v(x, y)\ \mathrm{dVol}(x, y) \\ \text{subject to} & |\nabla_1 v(x, y)| \leq 1 \text{ in } \{(x, y) \ \mid \ x \neq y\} \\ & |\nabla_2 v(x, y)| \leq 1 \text{ in } \{(x, y) \ \mid \ x \neq y\} \\ & v(x, y) \leq 0 \text{ on } \{(x, y) \ \mid \ x = y\} \end{array}} \tag{S8}$$

The problem (S8) clearly resembles problem (12). Accordingly, the proof Theorem 6.3 (just as the proof of Theorem 3.2, Supplemental 3) will consist in using compactness and show all limit points of the sequence U_α as $\alpha \to 0$ have to be just $d(x, y)$.

Theorem 6.1. *As $\alpha \to 0$, we have*

$$\|d(x, y) - U_\alpha(x, y)\|_{L^\infty(M\times M)} \to 0.$$

Proof. Let $\alpha_k \to 0$ be any sequence. The sequence $\{U_{\alpha_k}\}_k$ is uniformly Lipschitz, accordingly, there is a subsequence $\{U'_{\alpha_k}\}_k$ and a function $U_*(x, y)$ such that $U'_{\alpha_k} \to U_*$ uniformly in $M \times M$ as $k \to \infty$. We are going to show U_* must be the geodesic distance.

Indeed, let $\Phi(x, y) \to \mathbb{R}$ be any smooth admissible function for problem (12). Then, for any $\alpha > 0$ we have

$$-\int_{M\times M} U'_{\alpha_k}(x, y)\ \mathrm{dVol}(x, y)$$
$$\leq \alpha'_k \mathcal{E}_{M\times M}(U'_{\alpha_k}) - \int_{M\times M} U'_{\alpha_k}(x, y)\ \mathrm{dVol}(x, y)$$
$$\leq \alpha'_k s \mathcal{E}_{M\times M}(\Phi) - \int_{M\times M} \Phi(x, y)\ \mathrm{dVol}(x, y).$$

Taking the limit $\alpha'_k \to 0$ with the last inequality, it follows that

$$-\int_{M\times M} U_*(x, y)\ \mathrm{dVol}(x, y)$$
$$\leq -\int_{M\times M} \Phi(x, y)\ \mathrm{dVol}(x, y).$$

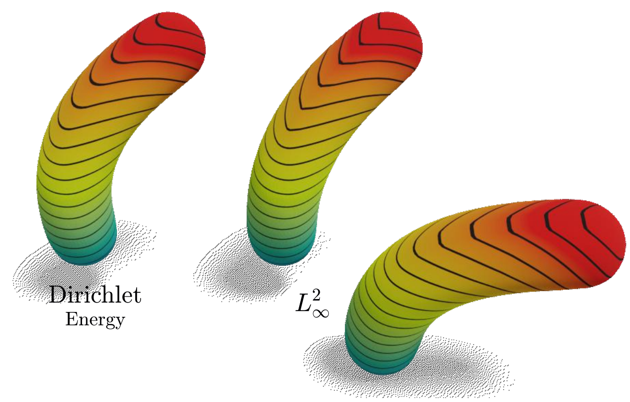

Figure 2: Non-quadratic regularizer example. We compare the results between the quadratic Dirichlet energy (left) to using the squared L_∞ norm on two meshes with different orientations (right). See the text for details.

Since Φ is an arbitrary admissible function, it follows that $U_* = d(x, y)$. This proves that U_k converges uniformly to $d(x, y)$, and in turn, by the same argument as in the proof of Theorem 3.2 (Supplemental 3) that $U_\alpha \to d(x, y)$ as $\alpha \to 0$. □

7 NON-QUADRATIC REGULARIZERS

The functional $F(\xi, x)$ used for the regularizer term in the minimization problem (3) allows for quite general norms or powers of norms. Using a non-isotropic norm from the ambient space, one obtains F's that have no dependence on x but manifest behavior that is sensitive to the position and orientation of M. We illustrate this with some numerical experiments with

$$F(\xi, x) = \|\xi\|_\infty^2, \tag{S9}$$

which satisfies all of the assumptions for Theorems 3.1 and 3.2 (as discussed at the start of Supplemental 2). Although (S9) involves a square, it is different from a quadratic polynomial on the entries of ξ. In fact, F in (S9) is not differentiable for all ξ, this can be seen by writing F in terms of the components of the vector ξ, if $\xi^t = (\xi_1, \xi_2, \xi_3)$ then

$$\|\xi\|_\infty = \max\{\xi_1^2, \xi_2^2, \xi_3^2\}.$$

This is a convex function of (ξ_1, ξ_2, ξ_3), it is smooth in the open set $\{|\xi_i| \neq |\xi_j| \text{ if } i \neq j\}$, but it is not differentiable along the boundary of this set.

In Fig. 2, we see how the regularized geodesics with $\mathcal{E}$ using (S9) look like for different orientations. Observe the anisotropic effects as the pipe is rotated as well as the flatter level curves.

8 DISTANCES TO A FIXED SOURCE ADMM DERIVATION (SECTION 5.4)

In Section 5.4 we present the augmented Lagrangian used to derive the ADMM algorithm.

$$L(u,y,z) = -A_{\mathcal{V}}^T u + \frac{\alpha}{2}u^T W u + \sum_{f\in\mathcal{F}} \chi(|z_f| \le 1) + \sum_{f\in\mathcal{F}} a_f y_f^T((\mathrm{G}u)_f - z_f) + \frac{\rho\sqrt{A}}{2}\sum_{f\in\mathcal{F}} a_f|(\mathrm{G}u)_f - z_f|^2,$$

where a_f is the area of the face f, $\rho \in \mathbb{R}$ is the penalty parameter, and $y \in \mathbb{R}^{3m}$ is the dual variable or Lagrange multiplier.

The ADMM algorithm iterates between three stages [Boyd et al. 2011, Section 3]: u-minimization, z-minimization, and updating the dual variable. Where using this formulation, both u and z have closed-form solutions.

The ADMM algorithm alternates between these three steps:

(1) $u^{k+1} = [\alpha W + \rho\sqrt{A}W_D]^{-1}[A_{\mathcal{V}} - \mathrm{D}y^k + \rho\sqrt{A}\mathrm{D}z^k]$
(2) $z_f^{k+1} = \mathrm{Proj}(\frac{1}{\rho\sqrt{A}}y_f^k + (\mathrm{G}u^{k+1})_f, \mathbb{B}^3)$ for all $f \in \mathcal{F}$
(3) $y^{k+1} = y^k + \rho\sqrt{A}(\mathrm{G}u^{k+1} - z^{k+1})$,

where $\mathrm{Proj}(z_f \in \mathbb{R}^3, \mathbb{B}^3)$ is equal to $z_f/|z_f|$ if $|z_f| > 1$, and z_f otherwise.

We consider our algorithms to have converged when $\|r^k\| \le \epsilon^{pri}$ and $\|s^k\| \le \epsilon^{dual}$, where r^k and s^k are the primal and dual residuals, resp. And $\epsilon^{pri}, \epsilon^{dual}$ are the primal and dual feasibility tolerances, resp. These quantities can be computed as follows:

$$\begin{aligned} r^k &= \sqrt{M_{\mathcal{F}}}\mathrm{G}u^k - \sqrt{M_{\mathcal{F}}}z^k \\ s^k &= \rho\mathrm{D}(z^k - z^{k-1}) \\ \epsilon^{pri} &= \sqrt{3m}\epsilon^{abs}A + \epsilon^{rel}\sqrt{A}\max(\|\sqrt{M_{\mathcal{F}}}\mathrm{G}u^k\|, \|\sqrt{M_{\mathcal{F}}}z^k\|) \\ \epsilon^{dual} &= \sqrt{n}\epsilon^{abs}A + \epsilon^{rel}\sqrt{A}\|\mathrm{D}y\|. \end{aligned}$$

In all our experiments, we set $\epsilon^{abs} = 5 \cdot 10^{-6}, \epsilon^{rel} = 10^{-2}$, and $\rho = 2$. We define ρ, the residuals and feasibility tolerances such that they are scale-invariance, as explained in Section 7.1.

In addition, to accelerate the convergence, we also use the varying penalty parameter and over-relaxation, exactly as described in [Boyd et al. 2011, Sections 3.4.1, 3.4.3].

9 SYMMETRIC ALL-PAIRS ADMM DERIVATION (SECTION 6.2)

Our discrete optimization problem, as introduced in Section 6.2, is:

$$\begin{aligned} \text{Minimize}_U \quad & -A_{\mathcal{V}}^T U A_{\mathcal{V}} + \\ & \tfrac{1}{2}\alpha\,\mathrm{Tr}\left(M_{\mathcal{V}}\left(U^T W_D U + U W_D U^T\right)\right) \\ \text{subject to} \quad & |(\nabla U_{(i,\cdot)})_f| \le 1 \quad \text{for all } f \in \mathcal{F}, i \in \mathcal{V} \\ & |(\nabla U_{(\cdot,j)})_f| \le 1 \quad \text{for all } f \in \mathcal{F}, j \in \mathcal{V} \\ & U_{i,i} \le 0 \quad \text{for all } i \in \mathcal{V}, \end{aligned}$$

where $X_{i,j}$ denotes the (i,j)-th element of a matrix X, $X_{(i,\cdot)}$ denotes the i-th row, and $X_{(\cdot,j)}$ the j-th column.

Our derivation is based on the consensus problem [Boyd et al . 2011, Section 7], where we split U into two variables $X, R \in \mathbb{R}^{n\times n}$ to represent the gradient along the columns and rows, and use a consensus auxiliary variable $U \in \mathbb{R}^{n\times n}$ to ensure consistency. We also add two auxiliary variables $Z, Q \in \mathbb{R}^{3m\times n}$ representing the gradients along the columns and rows, i.e., $\mathrm{G}X, \mathrm{G}R$. We enforce the diagonal constraint on the consensus variable U to avoid solving huge linear systems. This leads to the following optimization problem:

$$\begin{aligned} \text{Minimize}_U \quad & -\tfrac{1}{2}A_{\mathcal{V}}^T X A_{\mathcal{V}} - \tfrac{1}{2}A_{\mathcal{V}}^T R A_{\mathcal{V}} + \\ & \tfrac{1}{2}\alpha\,\mathrm{Tr}\left(M_{\mathcal{V}}\left(X^T W_D X + R^T W_D R\right)\right) + \\ & \sum_{f\in\mathcal{F}}\sum_{i\in\mathcal{V}} \chi(|(Z_{(\cdot,i)})_f| \le 1) + \\ & \sum_{f\in\mathcal{F}}\sum_{i\in\mathcal{V}} \chi(|(Q_{(\cdot,i)})_f| \le 1) \\ \text{subject to} \quad & (\mathrm{G}X_{(\cdot,i)})_f = (Z_{(\cdot,i)})_f \quad \text{for all } f \in \mathcal{F}, i \in \mathcal{V} \\ & (\mathrm{G}R_{(\cdot,i)})_f = (Q_{(\cdot,i)})_f \quad \text{for all } f \in \mathcal{F}, i \in \mathcal{V} \\ & X = U \\ & X = U \\ & R = U^T \\ & U_{i,i} \le 0 \quad \text{for all } i \in \mathcal{V} \\ & U \ge 0, \end{aligned}$$

where $\chi(Z_{(\cdot,i)})_f| \le 1) = \infty$ if $Z_{(\cdot,i)})_f| > 1$ and 0 otherwise. The corresponding augmented Lagrangian is:

$$\begin{aligned} L(U,Y,Z) = & -\tfrac{1}{2}A_{\mathcal{V}}^T X A_{\mathcal{V}} - \tfrac{1}{2}A_{\mathcal{V}}^T R A_{\mathcal{V}} + \\ & \tfrac{1}{2}\alpha\,\mathrm{Tr}\left(M_{\mathcal{V}}\left(X^T W_D X + R^T W_D R\right)\right) + \\ & \sum_{f\in\mathcal{F}}\sum_{i\in\mathcal{V}} \chi(|(Z_{(\cdot,i)})_f| \le 1) + \\ & \sum_{f\in\mathcal{F}}\sum_{i\in\mathcal{V}} \chi(|(Q_{(\cdot,i)})_f| \le 1) + \\ & \mathrm{Tr}\left(M_{\mathcal{V}}\left(Y^T M_{\mathcal{F}}(\mathrm{G}X - Z) + S^T M_{\mathcal{F}}(\mathrm{G}R - Q)\right)\right) + \\ & \tfrac{\rho_1\sqrt{A}}{2}\mathrm{Tr}\left(M_{\mathcal{V}}(\mathrm{G}X - Z)^T M_{\mathcal{F}}(\mathrm{G}X - Z)\right) + \\ & \tfrac{\rho_1\sqrt{A}}{2}\mathrm{Tr}\left(M_{\mathcal{V}}(\mathrm{G}R - Q)^T M_{\mathcal{F}}(\mathrm{G}R - Q)\right) + \\ & \mathrm{Tr}\left(H^T(X - U)M_{\mathcal{V}}\right) + \mathrm{Tr}\left(K^T(R - U^T)M_{\mathcal{V}}\right) + \\ & \mathrm{Tr}\left(H^T(X - U)M_{\mathcal{V}}\right) + \\ & \tfrac{\rho_2\sqrt{A^{-1}}}{2}\mathrm{Tr}\left((X - U)^T M_{\mathcal{V}}(X - U)M_{\mathcal{V}}\right) + \\ & \tfrac{\rho_2\sqrt{A^{-1}}}{2}\mathrm{Tr}\left((R - U^T)^T M_{\mathcal{V}}(R - U^T)M_{\mathcal{V}}\right), \end{aligned}$$

where $\rho_1, \rho_2 \in \mathbb{R}$ are the penalty parameters, and $Y, S \in \mathbb{R}^{3m\times n}$, $H, K \in \mathbb{R}^{n\times n}$ are the dual variables.

The ADMM algorithm for this optimization problem consists of three stages. In the first stage, we optimize for Z, R. In the second step, we minimize the auxiliary variables Z, Q, U. Finally, in the third step, we update the dual variables added in the augmented Lagrangian.

(1)

$$\begin{aligned} X^{k+1} = & \left((\alpha + \rho_1\sqrt{A})W_D + \rho_2\sqrt{A^{-1}}M_{\mathcal{V}}\right)^{-1} \\ & \left(\tfrac{1}{2}A_{\mathcal{V}}A_{\mathcal{V}}^T M_{\mathcal{V}}^{-1} - \mathrm{D}Y^k + \right. \\ & \left. \rho_1\sqrt{A}\sqrt{A}\mathrm{D}z^k - M_{\mathcal{V}}H^k + \rho_2\sqrt{A^{-1}}M_{\mathcal{V}}U^k\right) \end{aligned}$$

$$\begin{aligned} R^{k+1} = & \left((\alpha + \rho_1\sqrt{A})W_D + \rho_2\sqrt{A^{-1}}M_{\mathcal{V}}\right)^{-1} \\ & \left(\tfrac{1}{2}A_{\mathcal{V}}A_{\mathcal{V}}^T M_{\mathcal{V}}^{-1} - \mathrm{D}S^k + \right. \\ & \left. \rho_1\sqrt{A}\mathrm{D}Q^k - M_{\mathcal{V}}K^k + \rho_2\sqrt{A^{-1}}M_{\mathcal{V}}U^{kT}\right) \end{aligned}$$

(2) $(Z^{k+1}_{(\cdot,i)})_f =$
$\text{Proj}\left(\frac{1}{\rho_1\sqrt{A}}(Y^k_{(\cdot,i)})_f + (\text{G}X^{k+1}_{(\cdot,i)})_f, \mathbb{B}^3\right)$ for all $i \in \mathcal{V}, f \in \mathcal{F}$
$(Q^{k+1}_{(\cdot,i)})_f =$
$\text{Proj}\left(\frac{1}{\rho_1\sqrt{A}}(S^k_{(\cdot,i)})_f + (\text{G}R^{k+1}_{(\cdot,i)})_f, \mathbb{B}^3\right)$ for all $i \in \mathcal{V}, f \in \mathcal{F}$
$U^{k+1} = \max\left(\frac{H^k + K^{kT}}{2\rho_2\sqrt{A^{-1}}} + \frac{X^{k+1}+R^{kT}}{2}, 0\right)$
$U^{k+1}_{i,i} = 0$ for all $i \in \mathcal{V}$

(3) $Y^{k+1} = Y^k + \rho_1\sqrt{A}(\text{G}X^{k+1} - z^{k+1})$
$S^{k+1} = S^k + \rho_1\sqrt{A}(\text{G}R^{k+1} - Q^{k+1})$
$H^{k+1} = H^k + \rho_2\sqrt{A^{-1}}(X^{k+1} - U^{k+1})$
$K^{k+1} = K^k + \rho_2\sqrt{A^{-1}}(R^{k+1} - U^{kT})$

Similarly to Section 5.4, the first steps include solving a linear system with the same coefficient matrix, which can be pre-factored to accelerate the computation.

We consider our algorithms to have converged when $\|r^k\| \le \epsilon^{pri}$ and $\|s^k\| \le \epsilon^{dual}$, where r^k and s^k are the primal and dual residuals, resp. And $\epsilon^{pri}, \epsilon^{dual}$ are the primal and dual feasibility tolerances, resp. These quantities can be computed as follows:

$$\begin{aligned} r^k &= \sqrt{M_\mathcal{F}}\text{G}u^k - \sqrt{M_\mathcal{F}}z^k \\ s^k &= \rho\text{D}(z^k - z^{k-1}) \\ \epsilon^{pri} &= \sqrt{3m}\epsilon^{abs}A + \epsilon^{rel}\max(\|\sqrt{M_\mathcal{F}}\text{G}u^k\|, \|\sqrt{M_\mathcal{F}}z^k\|) \\ \epsilon^{dual} &= \sqrt{n}\epsilon^{abs}A^2 + \epsilon^{rel}\|\sqrt{M_\mathcal{F}}\text{D}Y\| \end{aligned}$$

and equivalently for R, Q, S. The residuals for the consensus part are as follows:

$$\begin{aligned} r^k_1 &= M_\mathcal{V}(X^k - U^k)M_\mathcal{V} \\ r^k_2 &= M_\mathcal{V}(R^k - U^{Tk})M_\mathcal{V} \\ s^k &= \rho_2 M_\mathcal{V}(U^k - U^{k-1})M_\mathcal{V} \\ \epsilon^{pri}_1 &= \sqrt{n}\epsilon^{abs} + \epsilon^{rel}\max(\|M_\mathcal{V}X^kM_\mathcal{V}\|, \|\sqrt{M_\mathcal{F}}z^k\sqrt{M_\mathcal{V}}M_\mathcal{V}U^kM_\mathcal{V}\|) \\ \epsilon^{pri}_2 &= \sqrt{n}\epsilon^{abs}\sqrt{A^3} + \epsilon^{rel}\max(\|M_\mathcal{V}R^kM_\mathcal{V}\|, \|M_\mathcal{V}U^{Tk}M_\mathcal{V}\|) \\ \epsilon^{dual} &= \sqrt{n}\epsilon^{abs}A + \frac{\epsilon^{rel}}{2}(\|\sqrt{M_\mathcal{V}}H\sqrt{M_\mathcal{V}}\| + \|\sqrt{M_\mathcal{V}}K\sqrt{M_\mathcal{V}}\|). \end{aligned}$$

We set $\epsilon^{abs} = 10^{-6}, \epsilon^{rel} = 2 \cdot 10^{-4}$ and $\rho_1 = \rho_2 = 2$ in all our experiments. Note that both the penalty variables, the residuals and feasibility thresholds are defined to be scale-invariance , as explained in section 7.1.

In addition, to accelerate the convergence, we also use the varying penalty parameter and over-relaxation, exactly as described in [Boyd et al. 2011, Sections 3.4.1, 3.4.3].

10 ADDITIONAL RESULTS

10.1 Additional examples

Figure 3 shows more examples of our fixed source (Alg. 1) method for the meshes in Table 1, Section 5.4.

Table 1: Timings in seconds for the All-Pairs distance computation on the cat model, $|\mathcal{F}| = 3898$, Figure 10 (main paper).

	Heat - Symmetrized [sec]	Fixed-Source - Symmetrized [sec]	All-Pairs [sec]
(a)	0.77	101.625	1124.312
(b)	0.77	59.583	837.063
(c)	0.76	37.4745	794.9549

10.2 Representation error in a spectral reduced basis

Smoother functions are better represented in a reduced basis comprised of the eigenvectors of the Laplace-Beltrami operator. Namely, they require less basis functions for the same representation error. In Fig. 4 (left) We compare the representation error in a reduced basis of our approach, the heat method, and fast marching. Note that our approach, both the fixed source (Alg. 1) and the all-pairs (Alg 2.) formulations, achieves the lowest error (indicating that the functions are smoothest in this sense). Similarly, we compare the symmetric formulations by symmetrizing our fixed source method, the heat method and the Fast Marching results, see Fig. 4 (right). Here we project on the eigenvectors of the LB operator on the *product manifold*. Here as well we achieve a lower error than the alternatives. The experiment was done on the "pipe" mesh, where we computed the full distance matrix between all pairs of vertices. For Fig 4 (left) we projected each column of the distance matrix (i.e., the distance from a single source vertex), and computed the mean of the representation errors. For Fig 4 (right), we projected the full distance matrix on the eigenvectors of the LB operator on the product manifold.

10.3 Additional results on various triangulations

To further demonstrate the robustness of our algorithm, we show additional results on low-quality triangulations in Figure 5. The leftmost column corresponds to a uniform triangulation and the other three to non-uniform triangulations. Note that the results remain similar for the different triangulations.

10.4 Timings for the All-Pairs formulation

Table 1 shows the running times for computing the all-pairs distances on the cat model. We compare the heat method, computed using Geometry Central [Sharp et al. 2019] (using the precomputation speed-up), our fixed source formulation (Alg. 1) and our all-pairs approach (Alg. 2). Note that Alg. 2 has a higher memory overhead than Alg. 1, because we are working with large dense matrices. Therefore, in our non-optimized Matlab implementation we may run out of memory for large meshes. We believe that a more careful implementation can improve this considerably.

10.5 Quadratic Finite Elements

Piecewise linear elements are not good approximators of the geodesic distance near the source. Intuitively, for coarse meshing, instead of generating round isolines, PL elements lead to polygonal isolines, see e.g. the output on the disk in Fig. 6 (left). Our

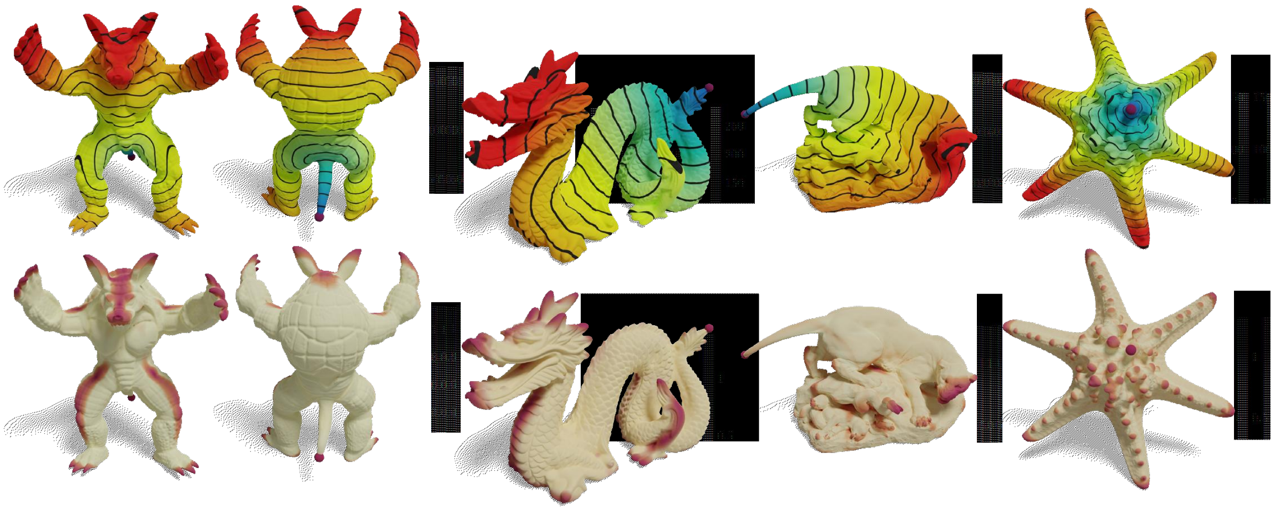

Figure 3: The distance isolines and gradient norm with Dirichlet regularization for various meshes.

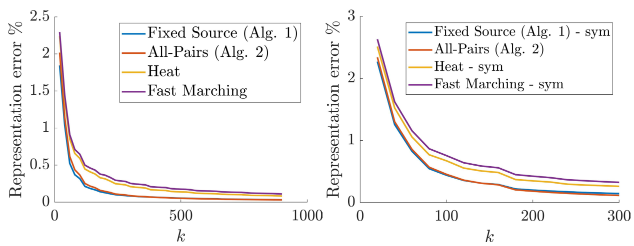

Figure 4: Comparison of the representation error of the Dirichlet regularized distances in a reduced spectral basis. See the text for details.

approach generalizes to piecewise quadratic elements in a straightforward way. Specifically, we replace the mass matrix, gradient and Laplacian with the corresponding matrices for quadratic elements [Boksebeld and Vaxman 2022, Appendix B]. The result is shown in Figure 6 (center). Note that the quadratic elements lead to a better approximation (compare with the analytical solution, Fig. 6 (right)).

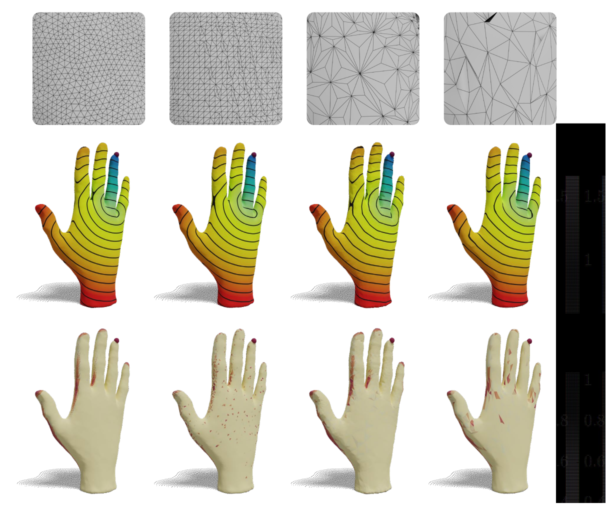

Figure 5: The regularized geodesic distance using the Dirichlet regularizer for various triangulations. For each triangulation, we display the connectivity (top), the isoline of the distance (middle) and the gradient norm, $|\nabla u|$ (bottom). Note that the results are qualitatively similar for all the triangulations.

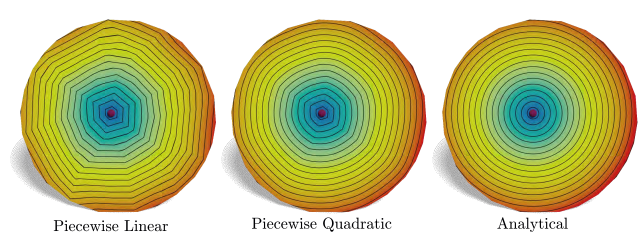

Figure 6: (left) Piecewise linear elements are not good approximators of geodsic distances near the source. (center) Our approach easily generalizes to quadratic elements. Note the improved accuracy (compare with the analytic solution (right)).